Advances in Materials Research, *Vol. 14, No. 4 (2025) 000-000*
https://doi.org/10.12989/amr.2025.14.4.000

Evaluate the effectiveness of die clearance and die radius on burr height and stress of aluminum AA1050 in progressive die by simulation and experiment

Tan Thanh Nguyen[a], Duong Van My[b], Truong Thanh Cong[c] and Pham Thi Hong Nga*

Faculty of Mechanical Engineering, Ho Chi Minh City University of Technology and Education, 01 Vo Van Ngan Street, Thu Duc ward, Ho Chi Minh City, 71307, Vietnam

(*Received February 7, 2023, Revised August 3, 2025, Accepted August 4, 2025*)

Abstract. Sheet metal forming is one of the most valuable processes in manufacturing. Its products are used in mechanical engineering, the auto industry, warehouses, civil engineering, and architecture. Shearing and forming are two of the primary operations in sheet metal processing. They are the first fundamental stage in processing sheet metal. The quality of the forming product is a manufacturing parameter. Shearing and forming processes, including progressive, die clearance, and radius, are the main factors influencing the quality. In this paper, the effects of die clearance and die radius on burr height and stress of aluminum are investigated by simulation and experiment. The findings revealed a direct correlation between die clearance and stress on the workpiece, with smaller clearance inducing higher stress and lower burr formation. The clearance exhibited minimal influence on stress and deformation. A 6% die clearance yielded the lowest burr height. Increasing the fillet radius mitigated stress concentration, diminished the critical cross-sectional area, and lessened deformation; however, it resulted in a less defined product shape.

Keywords: burr height; die clearance; die radius; progressive die; simulation

1. Introduction

Blanking and embossing are two standard sheet metal forming processes in the manufacturing industry. Blanking is a process of separating a metal blank into parts with the desired shape by applying a cutting force. Embossing, on the other hand, is a process of changing the shape of a metal blank by pressing the blank into a mold with the desired shape. Products created through blanking and embossing processes are found in various areas of life, ranging from simple household items to intricate components of automobiles and machinery.

Previous studies have focused on analyzing the effects of various factors on the quality of blanked products, including blanking force, blanking speed, mold shape, blank material, and other process parameters, such as the optimization of parameters during cold stamping (Xu *et al*. (2012), Pereira

* Associate Professor, E-mail: hongnga@hcmute.edu.vn
[a] Ph.D. Student, E-mail: tannt@hcmute.edu.vn
[b] Student, E-mail: 19144281@student.hcmute.edu.vn
[c] Ph.D., E-mail: congtt@hcmute.edu.vn

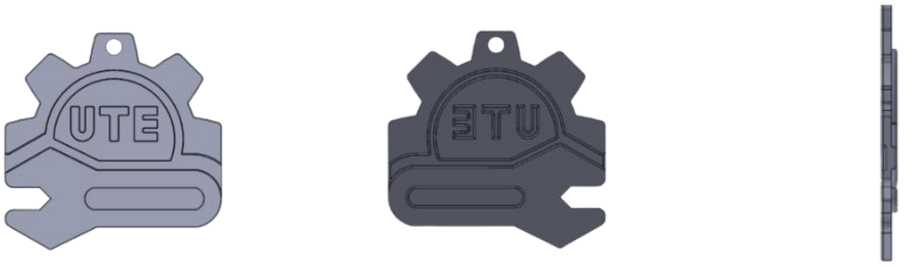

(a) Front view (b) Back view (c) Side view

Fig. 1 Product design

Table 1 Material data for AA1050 Bouchaâla *et al*. (2021) in this work

Parameters	Value
Density (kg/m^3)	2700
Strength coefficient (k) (MPa)	149
Strain hardening exponent (n)	0.287
Young Modulus (E) (GPa)	69
Poisson's ratio	0.33

et al. (2013), Chen *et al*. (2022)), simulate the deformation process (Azamirad *et al*. (2017), Nilsson *et al*. (2007), Ting *et al*. (2007)), optimization (Shaheen *et al*. (2020), Kuo *et al*. (2019), Wojtkowiak *et al*. (2019)), automated design processes (Lin *et al*. (2008), Cao *et al*. (2001), Silva *et al*. (2021), Bouchaâla (2021)).

However, detailed research on the effect of the clearance between the punch and die on the burr height during blanking and the effect of the corner radius on the product quality during forming is still limited. Although some studies have mentioned these factors, they often focus on specific cases or lack in-depth analysis of the mechanism of burr formation and the relationship between the corner radius and product quality indicators. This study aims to investigate the impact of the clearance between the punch and die on burr height during stamping, as well as the effect of the corner radius on product quality during forming.

2. Materials and Methods

2.1 Material

Table 1 displays the product's material. Fig. 1 depicts the product's design, including the forming and blanking procedure.

2.2 Deform 3D software

Deform 3D (Scientific Forming Technologies Corporation, Ohio, USA) is used to analyze metal forming, heat treatment, machining, and mechanical joining processes on the computer rather than the shop floor, using trial and error (Nitish *et al*. 2023).

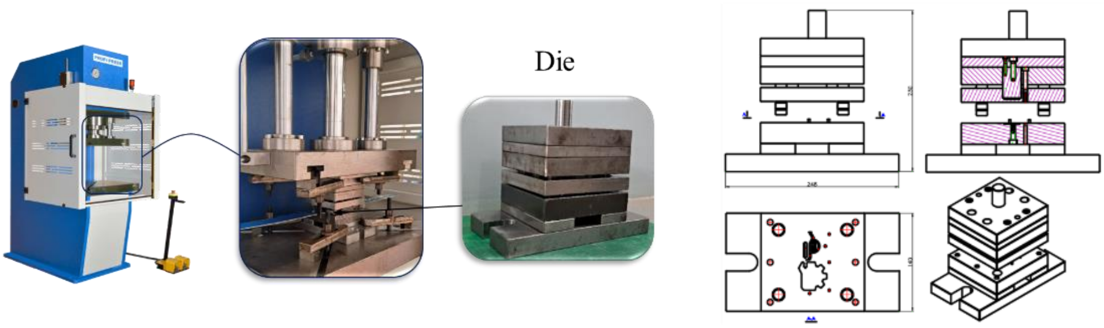

(a) Die assembly and die (b) Structure of die

Fig. 2 a) Profi Press PPCM-50 is used for the experiment

Table 2 Features and specifications of Profi Press PPCM-50

Specifications	Value	Unit
Force	50000	kg
Motor power	4	kW
Throat depth	265	mm
Working speed	6.3	mm/s
Approaching speed	32	mm/s
Return speed	42	mm/s
Maximum pressure	320	bar
Piston stroke	250	mm
Guides diameter	50	mm
Lower table size	700 x 450	mm
Upper table size	550 x 300	mm
Max. vertical light	400	mm
Working height	850	mm
Specifications	Value	Unit

2.3 Machine and die

Profi Press PPCM-50 (Schaijk, The Netherlands) with sheet metal die (Fig. 2) is used to experiment with the parameters in Table 2.

2.4 Experiment process

For blanking

Input the 3D CAD file (including the workpiece, punch, and die) in Deform 3D. Set up the position, dimension, parameter, material, meshing, and stepping. The left is the forming process, and the right is the shearing process (Fig. 3).

Shearing Process input parameter:

Material is AA 1050, mesh size is 100000, initial temperature is 35 °C, material thickness is

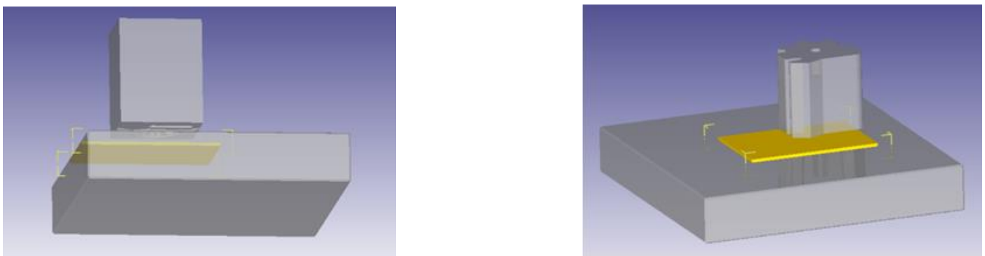

(a) From punch (b) Shearing punch

Fig. 3 Die structure

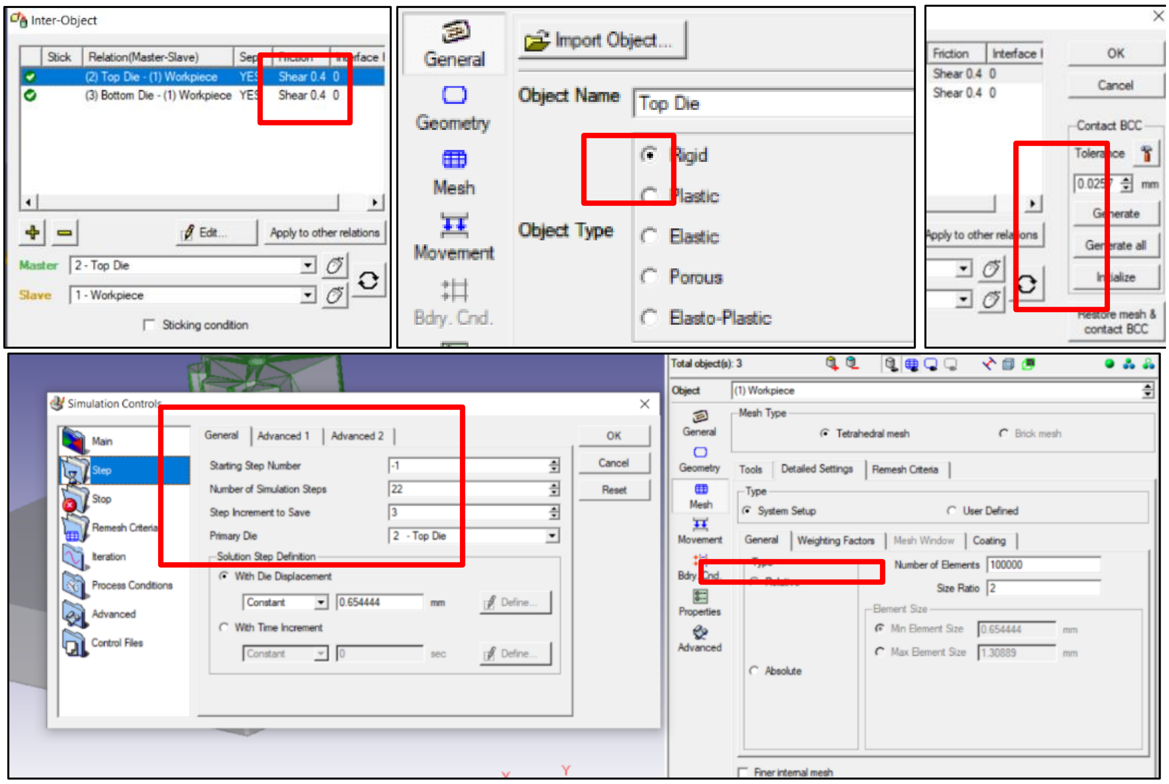

Fig. 4 Input parameter in Deform 3D

2mm, cutting speed is 350 mm/s, and stroke is 13 mm.

Variable: The die clearance is changed based on a formula:

U = a.t

Here

- U: die clearance (mm)
- t: thickness of material (mm)
- a: constant (a: 3%, 4%, 6%, 10%, 20%)

The parameter in Deform 3D is shown in Fig. 4:

- Rigid is used for the die and punch, and plastic is used for the workpiece

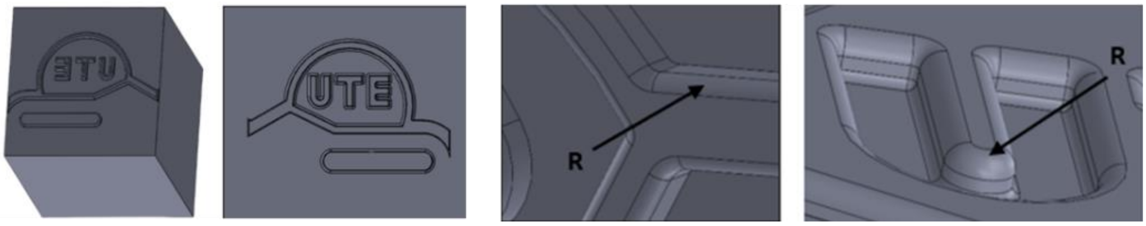

(a) Punch of forming tool (b) Radius of die (R)

Fig. 5 Punch of forming tool and radius of die (R)

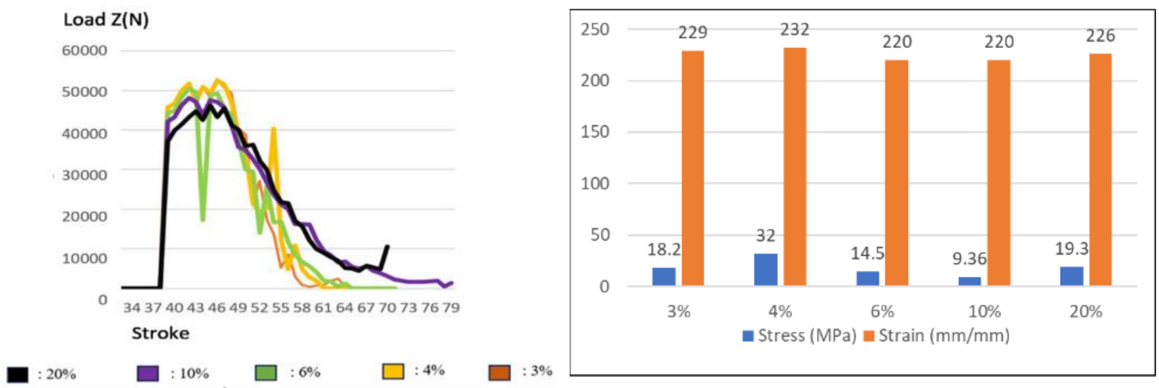

(a) Force and stroke in punch

(b) Effect of die clearance on stress and strain in simulation

Fig. 6 Force and stroke in punch

- With Die Displacement = Min Element Size / 3
- Number of Simulation Steps = Punch stroke / With Die Displacement
- Step Increment to save: save every three steps.
- Experiment with varying punch sizes while maintaining a constant die size. Compare and analyze the resulting changes in effective stress and effective strain. Observe and comment on the product variations when the clearance is set at 3%, 4%, 6%, 10%, and 20%.

For forming

The billet, die, and embossing punch parameters depicted in Fig. 5 were imported into DEFORM as a blanking process. The strain and stress distribution were investigated by modifying the fillet radius of the punch and die, as illustrated in Fig. 5.

3. Results and discussion

3.1 Effect of die clearance on the burr height of the product

The results of the effect of die clearance at 3%, 4%, 6%, 10%, and 20% to force (Z axis) are shown in Fig. 6a.

Observing the results in Fig. 6a, we notice that the applied force is not uniformly distributed and depends on the specific deformation zone of the material, corresponding to the elastic, plastic, and

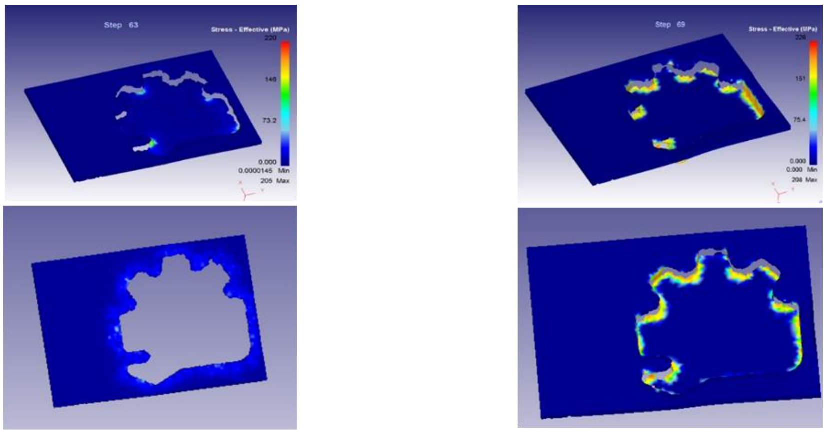

(a) 3%, 4%, and 6% (b) 20%

Fig. 7 Section of the shearing part of 3%, 4%, 6% and 20%

fracture regions of the material. In the force-displacement diagrams for 3%, 4%, and 6% deformation, it is observed that the final force values are zero. At that point, the workpiece has been completely separated from the original strip, so the force acting on the punch becomes zero. However, in the remaining two simulation cases of 10% and 20%, the force-displacement diagrams show that there is still a force acting at the final stroke of the punch, indicating that the product will not be separated from the strip. The force tends to decrease as the die clearance increases due to the stress distribution along the cutting edge. In the case of a 3% die clearance, according to Fig. 6b, the relationship between strain and stress shows that the stress increases significantly in the initial steps as the material deformation begins to change. Afterward, it remains relatively constant within a certain range to fracture the subsequent deformation zones. The stress becomes zero when the material deformation is complete

A general equation to show how to calculate Strain and Stress using data from 3D Deform.

Strain effective: $$\bar{\epsilon} = \frac{\sqrt{2}}{3}.\sqrt{(\epsilon_1-\epsilon_2)^2 + (\epsilon_2-\epsilon_3)^2 + (\epsilon_3-\epsilon_1)^2} \quad (1)$$

Stress effective: $$\bar{\sigma} = \frac{\sqrt{2}}{3}.\sqrt{(\sigma_1-\sigma_2)^2 + (\sigma_2-\sigma_3)^2 + (\sigma_3-\sigma_1)^2} \quad (2)$$

Following the simulation, the effectiveness of die clearance in two scenarios 10% and 20% was evaluated, and experiments on three cases, 3%, 4%, and 6%. Fig. 7 reveals that the 6% case exhibited the lowest maximum strain. This indicates that the material experienced the least strain or critical step-by-step strength in the 6% case. During the cutting process, higher material strain correlates with increased burr length. Furthermore, the 6% case demonstrated the lowest stress, resulting in minimal material deformation. The influence of die clearance on burr height is illustrated in Fig. 8. The results clearly show a positive correlation between die clearance and burr height Yatsun *et al*. (2019), Ortiz *et al*. (2007), Yamashita *et al*. (2021), Rizk *et al*. (2024).

3.2 Effect of the die radius on the stress of the forming product

By varying the die radius R from 0.05 mm to 0.6 mm in increments of 0.1 mm, simulation results indicated that a radius of 0.2 mm resulted in the lowest strain and stress values

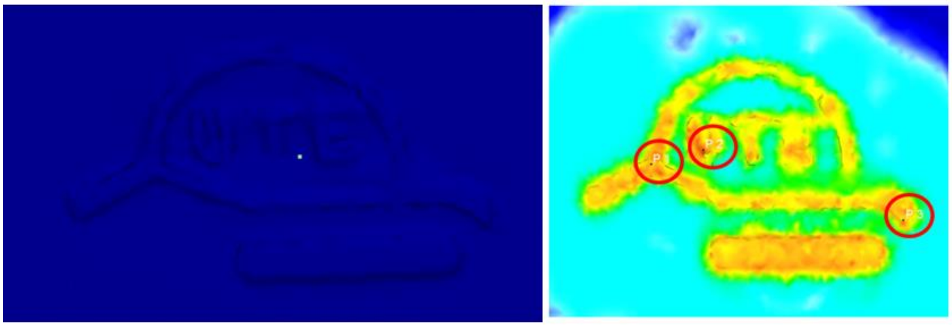

Fig. 9 The deformation behavior of the blank during the forming process, with a focus on the three points P1, P2, and P3 that exhibit the most severe stress concentration

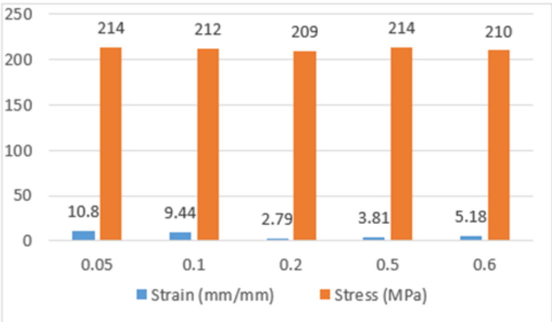

(a) Graph showing the correlation between strain and stress as the die clearance between the punch and die

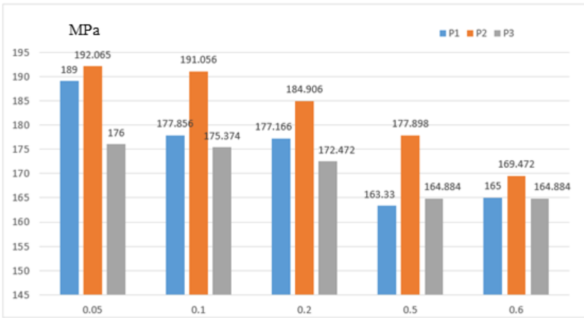

(b) Stress distribution at three critical points, P1, P2, and P3, for different die clearance

Fig. 10 The correlation between strain and stress as the die clearance between the punch and die

Fig. 11 Results from the forming experiment. a) initial blank and the stamped part, b) dimensional inspection, and c) final product."

Fig. 10a demonstrates a direct correlation between the corner radius R and the stress at the inspected points: the smaller the radius, the higher the stress. This is attributed to increased stress concentration on the blank as the clearance decreases. Experimental results (Fig. 10b), obtained using a 6% punch-die clearance for blanking and a 0.2 mm corner radius for the punch and die, confirm the design parameters: accurate dimensions, no warping, clear embossed shape without tears in critical stress areas, and a smooth cut edge (Fig. 11) Tekiner *et al*. (2006), Naranje and Kumar (2011).

4. Conclusions

Simulation results for AA1050 material deformation align with experimental data. Key findings include:

In shearing, larger die clearance led to increased burr height (peaking at 201.8 μm for a 20% thickness) and reduced stress concentration.

In embossing, larger die clearance resulted in lower applied force and stress concentration, mitigating the risk of failure but compromising the clarity of the formed features.

These findings enable the identification of potential failure zones during the design phase, saving time and costs. By utilizing simulation software with input parameters such as material models, punch and die deformation models, boundary conditions, and process parameters, the need for repeated physical trials is eliminated. This allows for efficient parameter modification at a low cost. Consequently, combining simulation-based analysis with practical experience optimizes production efficiency, reducing time and costs.

Acknowledgments

We would like to express our deep gratitude to Ho Chi Minh City University of Technology and Education and the Material Testing Laboratory for sponsoring the machines and equipment for the experiment. Additionally, we would like to thank the reviewers and editors for their constructive comments and suggestions, which have helped us improve our work.

References

Azamirad, G. and Arezoo, B. (2017), "Topology optimization of stamping die components using evolutionary structural optimization method", *Proc. Inst. Mech. Eng. B. J. Eng. Manuf.*, **231**(4). https://doi.org/10.1177/0954405415597630.

Bouchaâla, K., Ghanameh, M.F., Faqir, M., Mada, M. and Essadiqi, E. (2021), "Numerical investigation of the effect of punch corner radius and die shoulder radius on the flange earrings for AA1050 and AA1100 aluminum alloys in cylindrical deep drawing process", *Heliyon*, **7**(4).

Cao, J., Kinsey, B.L., Yao, H., Viswanathan, V. and Song, N. (2001), "Next generation stamping dies - controllability and flexibility", *Robot. Comput. Integr. Manuf.*, **17**(1-2). https://doi.org/10.1016/S0736-5845(00)00036-3.

Chen, L.W. and Yeh, C.T. (2022), "Development of a real-time failure detection system for stamping die", *Int. J. Adv. Manuf. Technol.*, **120**(7-8). https://doi.org/10.1007/s00170-022-09055-w.

da Silva, J.C., da Silva, F.J.G., Campilho, R.D.S.G., de Sá, J.C.V. and Ferreira, L.C.R.N.P. (2021), "A model for productivity improvement on machining of components for stamping dies", *Int. J. Ind. Eng. Manage.*, **12**(2). https://doi.org/10.24867/IJIEM-2021-2-279.

Kuo, C.C., Lin, B.T. and Wang, W. (2019), "Optimization of microridge punch design for deep drawing process by using the fuzzy Taguchi method", *Int. J. Adv. Manuf. Technol.*, **103**(1-4). https://doi.org/10.1007/s00170-019-03515-6.

Lin, B.T. and Kuo, C.C. (2008), "Application of an integrated CAD/CAE/CAM system for stamping dies for automobiles", *Int. J. Adv. Manuf. Technol.*, **35**(9-10). https://doi.org/10.1007/s00170-006-0785-y.

Naranje, V. and Kumar, S. (2011), "AI applications to metal stamping die design", *Artif. Intell. Approaches, Tools, Appl.*, **411041**, 71-95.

Nilsson, A. and Birath, F. (2007), "Topology optimization of a stamping die", *Proceedings of the AIP Conference*, **908**, 449-454. https://doi.org/10.1063/1.2740852.

Ortiz, C.J. and Caturla, M. (2007), "Simulation of defect evolution in irradiated materials: Role of intracascade clustering and correlated recombination", *Phys. Rev. B Condens. Matter Mater.*, **75**(18), 1-11. https://doi.org/10.1103/PhysRevB.75.184101.

Pereira, M.P., Weiss, M., Rolfe, B.F. and Hilditch, T.B. (2013), "The effect of the die radius profile accuracy on wear in sheet metal stamping", *Int. J. Mach. Tools Manuf.*, **66**. https://doi.org/10.1016/j.ijmachtools.2012.11.001.

Raja, N. and Daniel, B.S.S (2023), "Microstructural and mechanical characteristics of hot worked homogenized AA7068 using 3D processing map and DEFORM-3D", *Mater. Today Commun.*, **36**, 106574. https://doi.org/10.1016/j.mtcomm.2023.10657

Rizk, J., Rachik, M. and Maillard, A. (2024), "Finite element simulation of the complete sheet metal blanking cycle: Effect of blanking clearance on force curve and cut edge quality", *Heliyon*, **10**(9), e30334. https://doi.org/10.1016/j.heliyon.2024.e30334.

Shaheen, W., Kanapathipillai, S., Mathew, P. and Prusty, B.G. (2020), "Optimization of compound die piercing punches and double cutting process parameters using finite element analysis", *Proceedings of the Institution of Mechanical Engineers*, *Part B: Journal of Engineering Manufacture*, **234**(1-2). https://doi.org/10.1177/0954405419855507.

Tekiner, Z., Nalbant, M. and Gürün, H. (2006), "An experimental study for the effect of different clearances on burr, smooth-sheared and blanking force on aluminium sheet metal", *Mater. Des.*, **27**(10), 1134-1138. https://doi.org/10.1016/j.matdes.2005.03.013.

Ting, D., Yuqi, L., Zhibing, Z. and Zhigang, L. (2007), "Fast FE analysis system for sheet metal stamping-FASTAMP", *J. Mater. Proc. Technol.*, **187-188**. https://doi.org/10.1016/j.jmatprotec.2006.11.074.

Wojtkowiak, D. and Talaśka, K. (2019), "Determination of the effective geometrical features of the piercing punch for polymer composite belts", *Int. J. Adv. Manuf. Technol.*, **104**(1-4). https://doi.org/10.1007/s00170-019-03746-7.

Xu, D., Chen, J., Tang, Y. and Cao, J. (2012), "Topology optimization of die weight reduction for high-strength sheet metal stamping", *Int. J. Mech. Sci.*, **59(**1). https://doi.org/10.1016/j.ijmecsci.2012.03.006.

Yamashita, T., Koga, N., Kawasaki, T., Morooka, S., Tomono, S., Umezawa, O. and Harjo, S. (2021), "Work hardening behavior of dual phase copper-iron alloy at low temperature", *Mater. Sci. Eng. A*, **819**, 41509. https://doi.org/10.1016/j.msea.2021.141509.

Yatsun, S.F. and Jatsun, A.S. (2019), "Criterion of the Rehabilitation Process Effectiveness on the Basis of Biomehatronic System ExoLite RehabTM", *IOP Conf. Ser. Mater. Sci. Eng.*, **476**(1). https://doi.org/10.1088/1757-899X/476/1/012026.

CC